RESEARCH ARTICLE

Macromolecular
Materials and Engineering
www.mme-journal.de

Multicolor Fluorescent Polymeric Actuator with Self-Sustained Oscillation Behavior

Beibei Zhan, Shuxin Wei, Zhengfang Hu, Hao Liu, Huiyu Qiu, Qingquan Liu, Wei Lu,* and Tao Chen**

Soft fluorescent polymeric films are receiving increasing attention in the fields of sensing, display, information encryption, and so on. However, a few attempts are conducted to heterogeneously integrate fluorescent polymeric films with other soft polymeric materials into topology-optimized architectures (e.g., bilayer and pattern), which may lead to as-yet-unimagined performance. Herein, the synthesis of novel multicolor fluorescent polymeric films is presented via dynamic lanthanide coordination, followed by the fabrication of bilayer actuators with unique self-sustained oscillation behavior. The polymeric films are prepared from polydimethylsiloxane (PDMS) oligomer containing 2,6-pyridinediimine ligands that can chelate with Eu^{3+}/Tb^{3+} ions to trigger vivid red/bluish green fluorescence via antenna effect. After being further interfacially engineered with pan paper, fluorescent bilayer actuators are prepared, which display reversible 2D/3D shape deformation in response to environmental temperature changes owing to the mismatch between thermal expansion abilities of two layers. Interestingly, when placing the bilayer actuator with one end fixed near a constant heat source, quite unique self-sustained oscillation behavior is observed, which encourages to explore their potential applications as dynamic alarming devices. The present study broadens the list of fluorescent polymeric films and suggests the huge potential of multimaterial integration to develop powerful functional materials with versatile uses.

1. Introduction

Soft fluorescent polymeric films (SFPFs) are of great importance in the fields of sensing, display, information encryption, and so on.[1–4] Over the past decades, a number of fluorescent polymeric films have been constructed by physically incorporating or chemically grafting lanthanide complexes,[5–9] organic fluorogens,[10–19] or luminescent nanoparticles[20–21] into polymer matrix. These recent advances have significantly enriched the list of SFPFs and widened their potential applications. For example, Tang and co-workers presented an SFPF-based humidity sensor by assembling aggregation-induced emission-active molecular rotors into a moisture-captured poly(acrylic acid) network, which could rapidly report the environmental humidity change in high spatial-temporal resolution.[22] Zhang and co-workers covalently immobilized the protoporphyrin IX as internal reference and fluorescein isothiocyanate as indicator onto cellulose acetate polymer to prepare amine-responsive cellulose-based ratiometric fluorescent films that enable real-time and visual detection of seafood freshness.[23] Pan and co-workers incorporated quantum dots into polydimethylsiloxane (PDMS) material to produce multistate tunable fluorescent polymer films suitable for high-level anti-counterfeiting uses.[24] However, compared with these numerous studies that primarily engineer homogeneous SFPFs to achieve improved properties and fascinating functions, a few attempts have been conducted to heterogeneously integrate SFPFs with other soft polymeric materials with disparate properties into topology-optimized architectures (e.g., bilayer and pattern), which may lead to as-yet-unimagined performance.[25–30]

Herein, we utilized lanthanide-ligand coordination[31–33] to construct multicolor fluorescent polymeric films, and further integrated them with pan paper via interfacial composition to produce novel bilayer polymer actuators with quite unique self-sustained oscillation behavior at given temperature. The soft fluorescent polymeric films were prepared by the coordination of the PDMS oligomer containing 2,6-pyridinediimine groups with such lanthanide ions as Eu^{3+} and Tb^{3+}. Their multicolor emission comes from the newly formed red/bluish green

---

B. Zhan, Prof. Q. Q. Liu
School of Materials Science and Engineering
Hunan Provincial Key Laboratory of Advanced Materials for New Energy Storage and Conversion
Hunan University of Science and Technology
Xiangtan 411201, China
E-mail: qqliu@hnust.edu.cn

B. Zhan, Prof. Q. Q. Liu
School of Chemistry and Chemical Engineering
Hunan University of Sciences and Technology
Xiangtan 411201, China

B. Zhan, S. Wei, Z. Hu, H. Liu, H. Qiu, Prof. W. Lu, Prof. T. Chen
Key Laboratory of Bio-Based Polymeric Materials Technology and Application of Zhejiang Province
Chinese Academy of Science
1219 Zhongguan West Road
Ningbo Institute of Material Technology and Engineering
Ningbo 315201, China
E-mail: luwei@nimte.ac.cn; tao.chen@nimte.ac.cn

The ORCID identification number(s) for the author(s) of this article can be found under https://doi.org/10.1002/mame.202000781.

DOI: 10.1002/mame.202000781

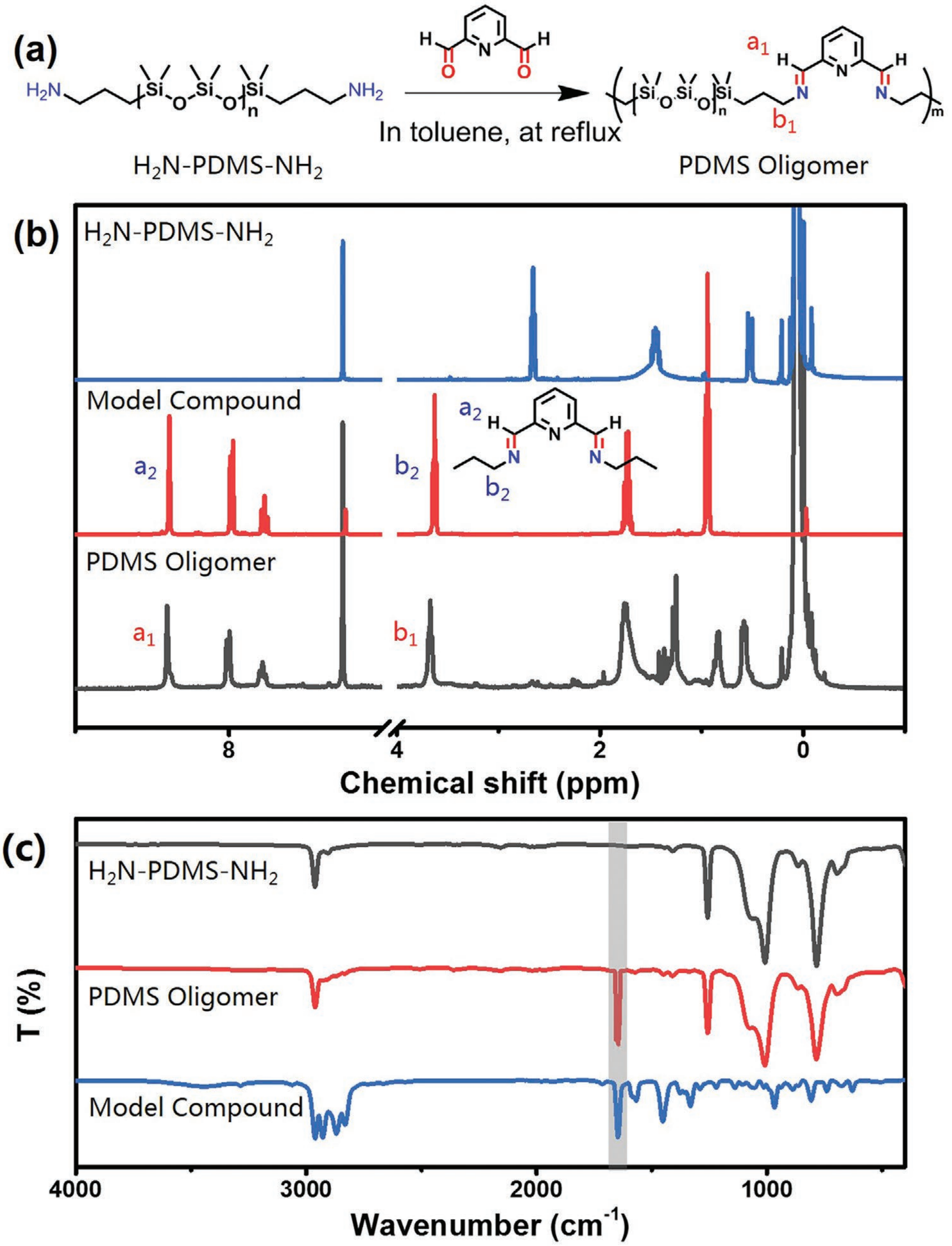

Figure 1. Synthesis of PDMS oligomer and its small-molecule model compound. a) Synthetic procedure of PDMS oligomer. b) Comparison of the ^{1}H NMR spectra of H_2N–PDMS–NH_2, PDMS oligomer, and the model compound. c) Comparison of the FI-IR spectra of H_2N–PDMS–NH_2, PDMS oligomer, and the model compound.

fluorescent Eu^{3+}/Tb^{3+} complexes. Interestingly, their emission colors could be facilely tuned by controlling the ratio of these two fluorescent centers. Upon integration of such polymeric films with commercially available pan paper via interfacial composition, fluorescent bilayer actuators were obtained. Owing to the mismatch of thermal expansion abilities between the SFPF and paper layers, the as-prepared bilayer actuator, when heated, would bend to paper side. Remarkably, when our bilayer actuator with one end fixed was placed near a given heat source with constant temperature, the free end would display interesting self-sustained oscillation movement. Their potential use as new-type alarming devices were further demonstrated by synergistically using dynamic oscillation movement and eye-catching fluorescence properties.

The key step to synthesizing such multicolor fluorescent polymeric films is the preparation of the PDMS oligomer containing 2,6-pyridinediimine groups. **Figure 1**a depicts its typical synthetic procedure. Briefly, the commercially available H_2N–PDMS–NH_2 was allowed to react with 2,6-pyridinedicarboxaldehyde at elevated temperature to give the PDMS oligomer as a brown viscous liquid. Its chemical structure was clearly verified by ^{1}H NMR (Figure 1b) and FI-IR spectra (Figure 1c). As a reference, its small-molecule model compound with the same 2,6-pyridinediimine chromophore was also prepared from the

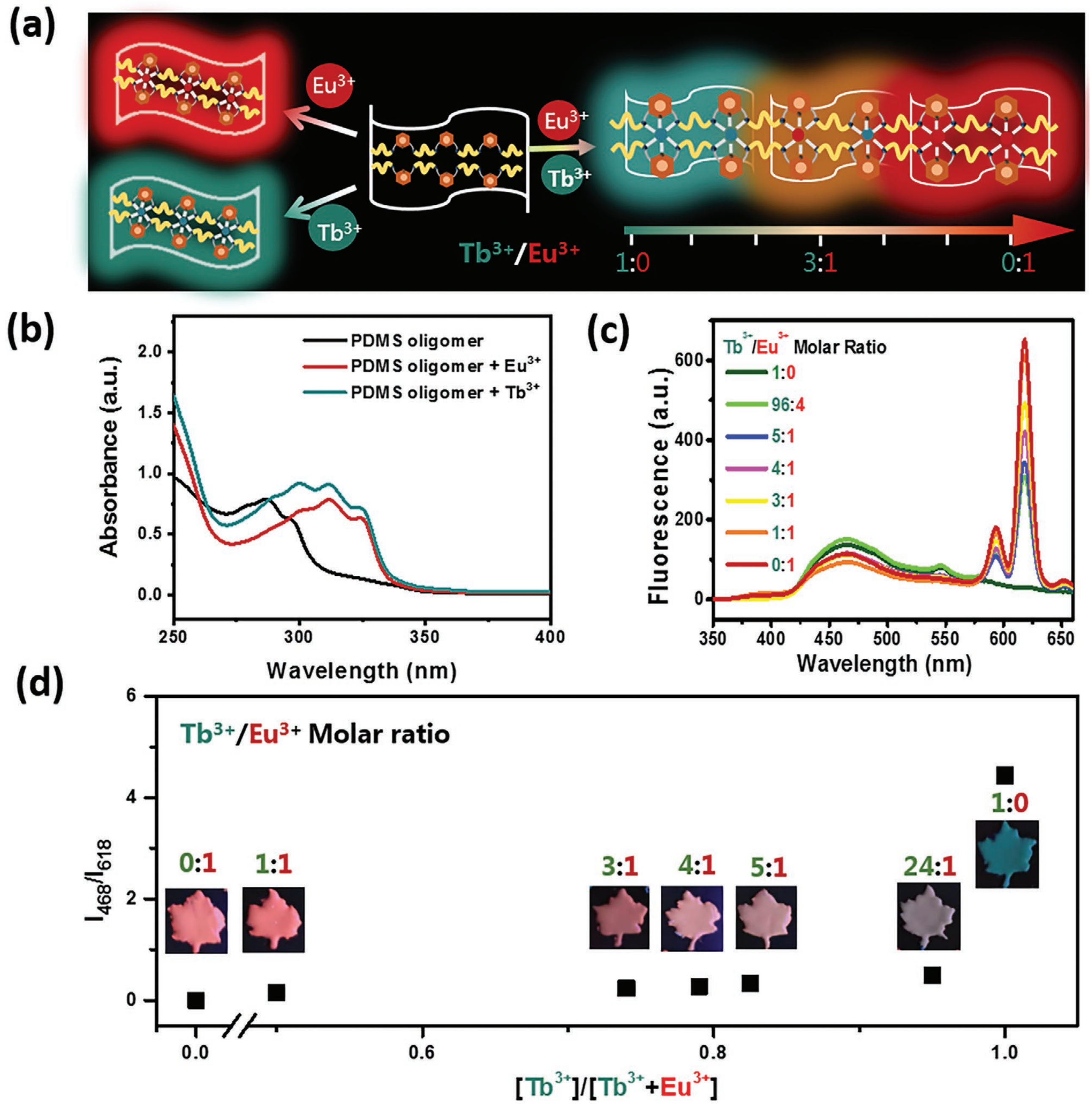

Figure 2. Preparation of the lanthanide coordinated multicolor fluorescent polymeric films. a) Illustration of the fluorescent polymeric films based on dynamic lanthanide coordination effect. b) Absorbance spectra of the PDMS oligomer solutions (in CH_2Cl_2) in the presence of Eu^{3+} or Tb^{3+}. c) Fluorescence spectra of the Eu^{3+} or Tb^{3+} coordinated polymeric films. d) Peak emission intensity ratio of the band centered at 468 nm to that around 618 nm.

aldimine condensation reaction between 2,6-pyridinedicarboxaldehyde and propylamine (Figure S1, Supporting Information), and characterized by ^1H NMR (Figure 1b), ^{13}C NMR (Figure S2, Supporting Information). Compared with $H_2N–PDMS–NH_2$, additional peaks around 1600 cm^{-1} appear in the FI-IR spectra (Figure 1c) of both PDMS oligomer and its small-molecule model compound, suggesting the successful incorporation of 2,6-pyridinediimine chromophore.

The multicolor fluorescent polymeric films were then prepared and studied. The as-prepared PDMS oligomer is nearly non-fluorescent under UV light illumination. Owing to the incorporation of 2,6-pyridinediimine ligands, the PDMS oligomer can chelate with such lanthanide ions as Eu^{3+} to form metal complexes (**Figure 2**a), as is evidenced by the appearance of new absorbance bands at longer wavelength in the UV–vis spectra (Figure 2b). The red-shifted UV–vis spectra could be ascribed to the presence of the metal-to-ligand (Eu^{3+}/Tb^{3+}-to-2,6-pyridinediimine) charge transfer (MLCT) state located at lower energy.[34] In order to investigate their luminescent properties in the dry solid state, the lanthanide-coordinated polymeric films were first prepared according to a modified version of the reported method.[35] In a typical experiment, the methanol solution of Eu^{3+} or Tb^{3+} salts (0.5 g mL^{-1}) was first added into the CH_2Cl_2 solution of PDMS oligomer (0.1 g mL^{-1}). The mixture was then concentrated and poured into the self-made polytetrafluoroethylene mold. After being dried at room temperature for 12 h, the mold was transferred into vacuum drying oven at 70 °C for 12 h. The fluorescent polymeric films were then peeled off from the PTFE mold for further use. Because of the efficient resonance energy transfer (the well-known antenna effect)[36] from the 2,6-pyridinediimine ligands as sensitizers to center Eu^{3+} ions, the obtained polymer film becomes red fluorescent upon Eu^{3+} coordination (Figure 2c,d). This result is further evidenced by the fluorescence spectral study of its small-molecule model compound (Figure S3, Supporting Information), which shows bright red light emission upon the addition of Eu^{3+} ions. Notably, upon Tb^{3+} introduction, emission intensity of the polymeric film at 465 nm increases, making it look bluish green under UV light (Figure 2d). This broad emission band centered at 465 nm is believed to come from the 2,6-pyridinediimine ligand. After chelating Tb^{3+}, its emission intensity increases because of the rigid molecular structure and then reduced molecular motion-caused nonradiative transition.[31,37,38] Besides Eu^{3+} and Tb^{3+}, other lanthanide ions such as (Sm^{3+}, Pr^{3+}, and Gd^{3+}) can also chelate with the PDMS oligomer to form fluorescent polymeric films (Figures S4 and S5, Supporting Information). Red and aquamarine fluorescent polymeric films were then obtained by mixing the PDMS oligomer with Eu^{3+} and Tb^{3+} ions (molar ratio of 2,6-pyridinediimine ligand to lanthanide ions is 2:1), respectively. As expected, when the red fluorescent Eu^{3+} complexes and aquamarine fluorescent Tb^{3+} complexes were simultaneously introduced, multicolor fluorescent polymeric films were obtained. As shown in Figure 2c,d, emission color of the films could be facilely modulated from red to bluish green by varying the molar ratio of these two lanthanide complexes. Fluorescence spectral studies reveal that the emission intensity of red band around 618 nm decreases, while the intensity of emission band around 468 nm increases upon increasing Tb^{3+}/Eu^{3+} molar ratio (Figure 2c).

Owing to the reversible nature of 2,6-pyridinediimine-lanthanide coordination interactions, as well as the viscous nature of PDMS matrix itself (**Figure 3**a), the fluorescent films were proved to have satisfying self-healing properties. To this end, Tb^{3+} and Eu^{3+}-coordinated films of various shapes were first prepared in self-made molds (Figure 3b,c). These films were then physically placed together at room temperature for 12 h. During this time, these separated two films would be gradually healed together by the dynamic dissolution and regeneration of 2,6-pyridinediimine-lanthanide complexes. The healed film could withstand its own weight and be lifted up, demonstrating their quite good self-healing properties at ambient conditions (Figure 3c).

Next, anisotropic bilayer actuators (**Figure 4**a) were prepared by interfacial composition of the fluorescent film and pan paper that is a very thin and soft paper (photos shown in Figure S6 in the Supporting Information) and usually used to weigh chemicals in the lab. The SEM image clearly demonstrates its bilayer structure (Figure 4b), in which the two layers are connected by the interpenetrating polymer chain entanglement. As shown in Figure 4d, the straight bilayer actuator with one end fixed will gradually bend and curl toward paper side after being heated to 100 °C, followed by gradual recovery when cooled to 30 °C. This directional actuation deformation is primarily caused by the mismatch between thermal expansion abilities of these two layers. Their actuation speed could be facilely modulated by varying the environmental temperature (Figure 4c). Remarkably, such thermotriggered shape deformation behavior was proved to be repeated for more than four cycles without large bending curvature loss (Figure S7, Supporting Information), suggesting the quite good actuating reversibility of our straight bilayer actuators. Furthermore, more powerful bilayer actuators with

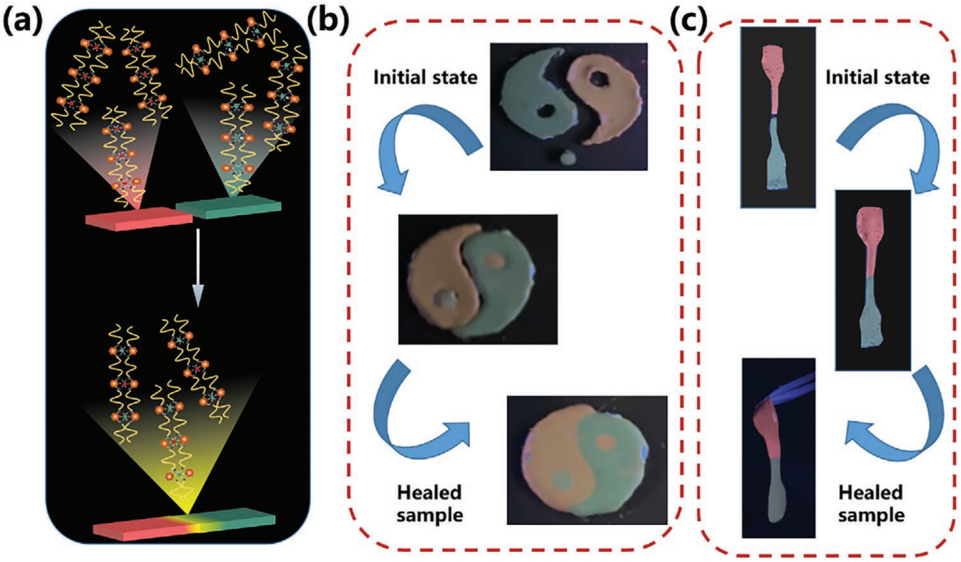

Figure 3. Study on the self-healing properties of the multicolor fluorescent polymeric films. a) The proposed self-healing mechanism. b,c) Photos showing the self-healing process of the fluorescent polymeric films.

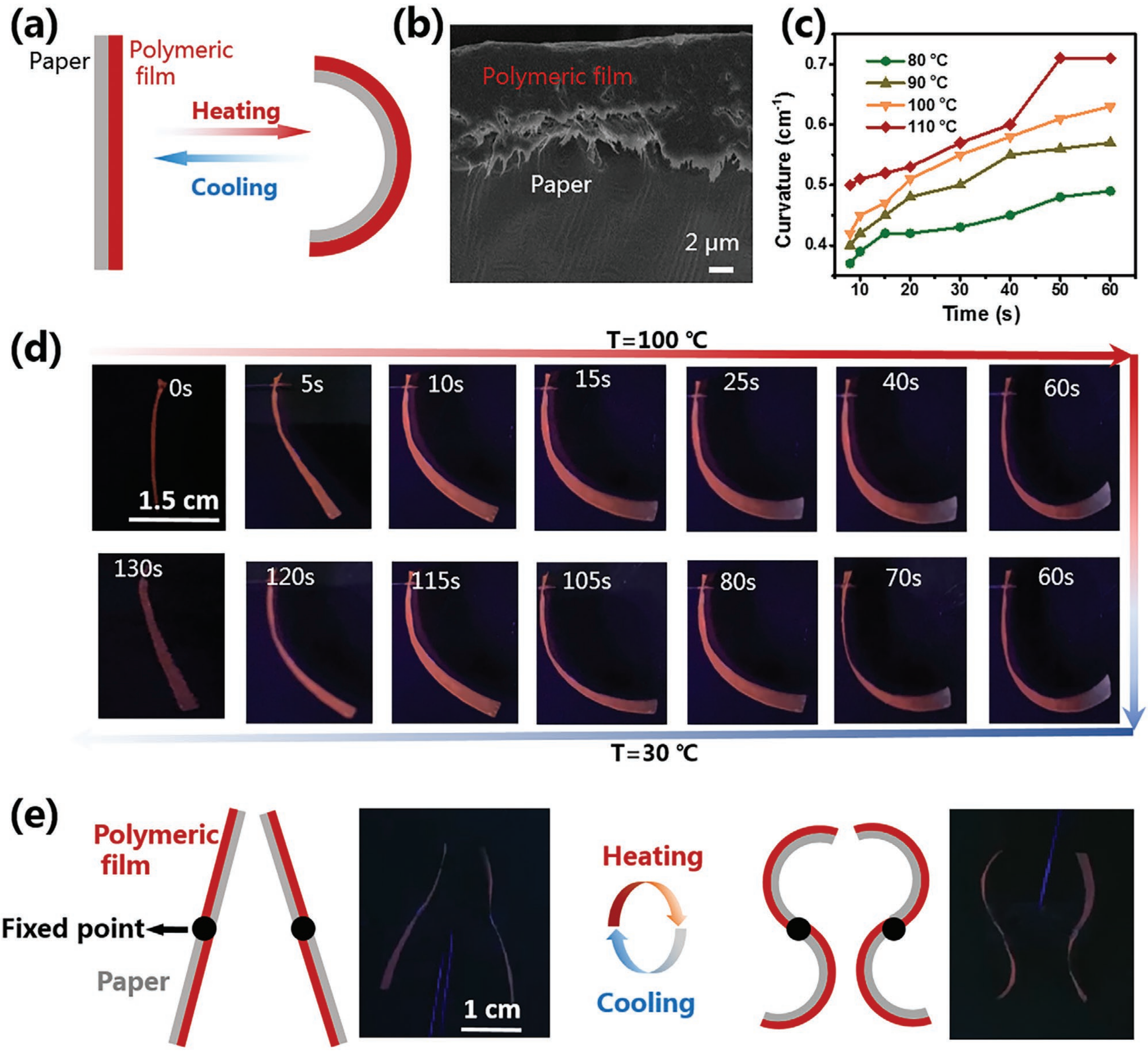

Figure 4. Fluorescent bilayer actuators. a) Illustration of the thermotriggered bilayer actuators. b) SEM image showing the cross-section structure of the bilayer actuators. c) Time-dependent bending curvatures at different temperature. d) Photos showing the thermoinduced shape change and recovery process. e) Actuators with complex 2D shape deformation.

complex 2D/3D shape deformation abilities were demonstrated. As can be seen from Figure 4e and Figure S8 (Supporting Information), the straight bilayer actuators of different length could be combined together to produce complex 2D shape deformation. As a result, meaningful information could be obtained at elevated temperature, suggesting its potential use for information encryption. Furthermore, the flower-shaped actuators prepared by bundling six bilayer structured petals together was first programmed as a dormant bud as the original state (Figure S9, Supporting Information). Upon temperature elevation to 100 °C, all of the petals steadily bend outward owing to the differential thermal expansion capabilities of the bilayer materials, resulting in gradual opening of the dormant bud to a blooming flower within 1 min. Bioinspired leaves with thermotriggered shape change were also prepared by interfacial composition of different lanthanide coordinated fluorescent films and pan papers (Figure S10, Supporting Information).

The most astonishing behavior of our bilayer actuator is that it could display the interesting self-sustained oscillation when placing such actuator with one end fixed near a given heat source with constant temperature (100 °C). As schemed in **Figure 5**a, upon exposure to the heat source, the larger expansion of film layer than paper layer will induce the actuator to bend toward the opposite direction of the heat source. When the actuating end moves to become far away from the heat source (state II), the actuator will be cooled to induce the quick shrinkage of the fluorescent film layer, thus causing it recover to the state III. Upon approaching the heat source again, the

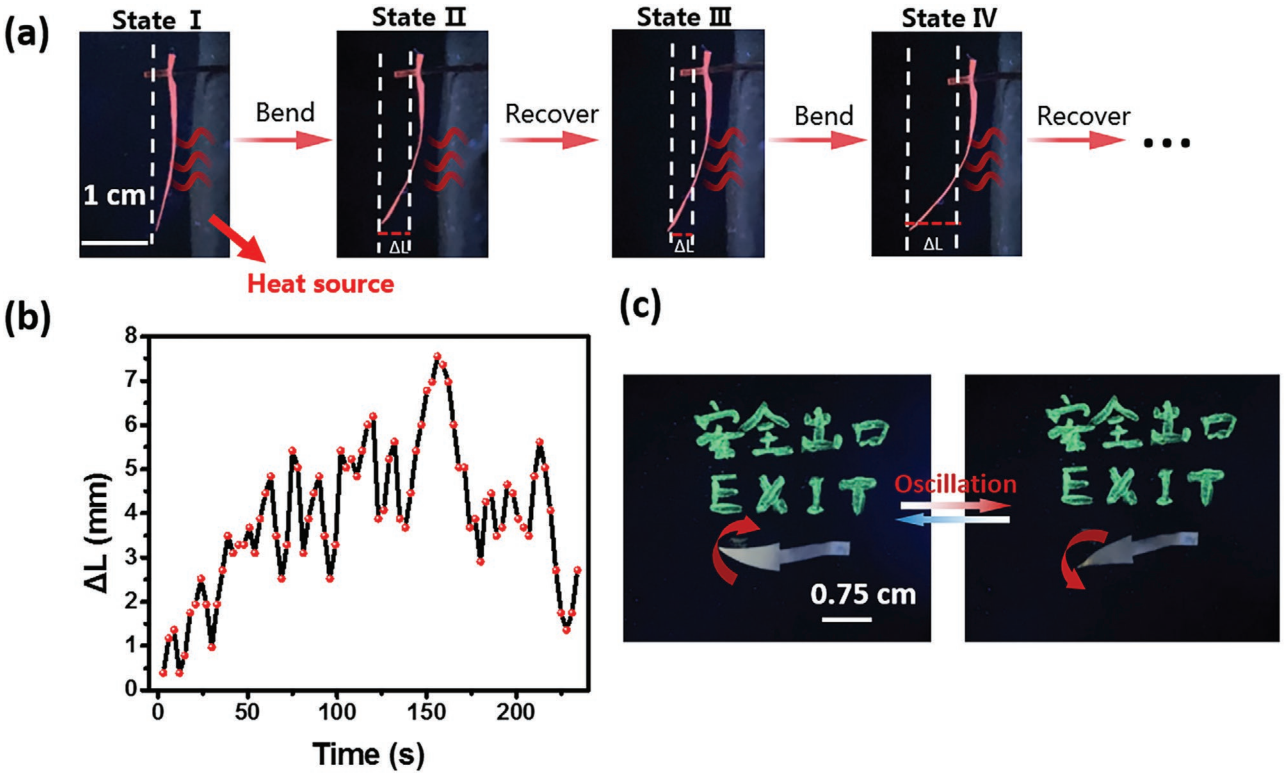

Figure 5. Bilayer actuators with self-sustained oscillation behavior that are placed near a given heat source with constant temperature (100 °C). a) Photos showing its self-sustained oscillation behavior. b) The relative displacement (ΔL) of the actuating end as a function of time. c) Its application as dynamic "EXIT" sign. Note that the arrow-shaped bilayer actuator was prepared by interfacial composition of Tb^{3+}-coordinated polymeric film and pan paper.

actuator will bend again to state IV. In this way, a dynamic and self-sustained oscillation behavior was realized (Movie S1, Supporting Information). Figure 5b shows the relative displacement (ΔL) of its actuating end as a function of time. The interesting self-sustained oscillation movement of the established actuators, together with their multicolor fluorescence properties, further encourages us to explore their potential use for dynamic alarming. One proof-of-concept example is shown in Figure 5c. An arrow-shaped bilayer actuator was first prepared and used as dynamic "EXIT" sign. As can be seen in Movie S2 (Supporting Information), upon approaching a given heat source, the designed "EXIT" sign displays self-sustained oscillation behavior, which is believed to be more efficient to attract people's attention than the currently used static "EXIT" sign. Besides, a dragonfly-shaped alarming device was also designed to remind workers to be careful of the hot pipelines in the factories (Figure S11 and Movie S3, Supporting Information).

2. Conclusion

In conclusion, we present a new type of PDMS-based multicolor fluorescent polymeric films, which can be interfacially composited with pan paper to produce dynamic bilayer actuators with self-sustained oscillation behaviors. The multicolor fluorescent films are prepared by the dynamic lanthanide (Eu^{3+}/Tb^{3+}) coordination of the PDMS oligomers containing 2,6-pyridinediimine ligands, which serve as efficient sensitizers to induce intense red and bluish green emission of center Eu^{3+}/Tb^{3+} ions. Based on the mismatch between thermal expansion abilities of the fluorescent films and pan paper, the as-prepared bilayer actuator could display directional actuation deformation to form various interesting 2D and 3D structures. Remarkably, unique self-sustained oscillation behavior was observed when placing our bilayer actuator with one end fixed near a given heat source with constant temperature, which could find versatile use as dynamic "EXIT" signs or alarming device to remind workers to be careful of the hot pipelines in the factories. The present study will broaden the list of polymeric actuators and inspire the future development of intelligent actuating systems.

3. Experimental Section

Materials: Poly(dimethylsiloxane) bis(3-aminopropyl) end-capped ($H_2N–PDMS–NH_2$, M_n = 900–1000) was purchased from Macleans Reagent Network. 2,6-Pyridinedicarbaldehyde, toluene, and acetic acid were purchased from Sinopharm Chemical Co., Ltd. $Eu(NO_3)_3$ and $Tb(NO_3)_3$ were purchased from Aldrich.

Characterization: ^1H NMR spectra of PDMS oligomer and the small molecule model compound, as well as ^{13}C NMR spectrum of model compound, were recorded on Bruker Advance AMX-400 Spectrometer. ATR-FT-IR spectra were recorded on a Micro FT-IR (Cary 660+620) instrument. Fluorescence spectra of the multicolor fluorescent polymeric films were measured by Hitachi F-4600 Spectrofluorometer equipped with a xenon (Xe) lamp (150 W). Cross-section morphology of the multicolor fluorescent polymeric films was performed by a field-emission scanning electron microscopy (SEM, S-4800, Hitachi). Digital photos were taken by a smartphone (iPhone 11).

Synthesis of the PDMS Oligomer: Under N_2 atmosphere, 2,6-pyridinedicarbaldehyde (1 g, 7.4 mmol) in anhydrous toluene (25 mL) was added to $H_2N–PDMS–NH_2$ (14.8 g, M_n = 900–1000) at room temperature (the stoichiometry of the NH_2 groups and the aldehyde groups is about 2:1). 150 µL acetic acid (catalyst) was further added and then heated to 130 °C for 12 h. After cooling to room temperature, the solvent was evaporated by a rotary evaporator at 45 °C. 5 mL CH_2Cl_2 was added to dissolve the residual product, and then 50 mL methanol was poured into the reactor. After being kept still for 30 min, brown viscous polymer precipitated. The PDMS oligomer (13 g) was then obtained after repeating the dissolution–precipitation–decantation process for two times and drying under vacuum at room temperature in a quite high yield (82.2%). The residual amino groups in the PDMS oligomer were calculated to be 56.9% according to the method described in Figure S12 (Supporting Information).

Synthesis of the Small Molecule Model Compound: Under N_2 atmosphere, excess n-propylamine (0.46 g, 4.8 mmol) and 2,6-pyridinedicarbaldehyde (0.5 g, 2.4 mmol) was added into absolute ethanol (20 mL). 100 µL acetic acid was then added as the catalyst. After being stirred at 65 °C for 4 h, the solvent was removed by rotary evaporation at 45 °C to give a reddish orange oil. The crude product was purified by column chromatography by using ethyl acetate/hexane (1/5, v/v) as the eluent. ^1H NMR (400 MHz, $CDCl_3$, δ): 8.40 (s, 2 H), 7.93 (d, 2 H), 7.78 (t, 1 H), 3.65 (t, 4 H), 1.72 (m, 4 H), 0.96 (t, 6 H).

Preparation of Multicolor Fluorescent Polymeric Films: The anhydrous methanol solution of these lanthanide salts (0.5 g mL^{-1}) was first prepared and then added into CH_2Cl_2 solution of the PDMS oligomer (0.1 g mL^{-1}). The mixture was concentrated and poured into the self-made polytetrafluoroethylene mold. After being dried at room temperature for 12 h, the mold was transferred into vacuum drying oven at 70 °C for 12 h. The fluorescent polymeric films were then peeled off from the PTFE mold for further use. As a control experiment, the methanol solution of Eu^{3+} or Tb^{3+} salts (0.5 g mL^{-1}) was mixed with CH_2Cl_2 solution of the PDMS without the ligands (0.1 g mL^{-1}). The mixture was concentrated and poured into the self-made polytetrafluoroethylene mold. However, after being dried, no fluorescent polymeric film was obtained. Instead, a viscous liquid with very weak fluorescence was obtained (Figure S13, Supporting Information). This control experiment clearly demonstrates that the amines on the PDMS indeed are poorer ligands and much worse energy harvesting chromophores than the 2,6-pyridinediimine ligand. These results further demonstrate that the 2,6-pyridinediimine ligands in the PDMS oligomer do play important roles in the preparation of fluorescent polymeric films.

Preparation of Bilayer Actuators: The concentrated CH_2Cl_2 solution of fluorescent polymeric films was dropped onto the pan paper and then evenly spread by the blade coating method. The bilayer actuators were then obtained after being dried in a drying oven at 70 °C for 2 h.

Supporting Information

Supporting Information is available from the Wiley Online Library or from the author.

Acknowledgements

The authors thank the financial support by the National Natural Science Foundation of China (21774138, 51773215, and 51778226), Key Research Program of Frontier Sciences, Chinese Academy of Sciences (QYZDB-SSW-SLH036), Youth Innovation Promotion Association of Chinese Academy of Sciences (2019297), Ningbo Scientific and Technological Innovation 2025 Major Project (2018B10057), and Key Laboratory of Marine Materials and Related Technologies, CAS (2020K05).

Author Contributions

B.B.Z., Q.Q.L., W.L., and T.C. conceived the experiments. B.B.Z., S.X.W., Z.F.H., H.L., H.Y.Q. performed the experiments. B.B.Z., Q.Q.L., W.L., S.X.W., Z.F.H., H.L., H.Y.Q., and T.C. cowrote the paper.

Conflict of Interest

The authors declare no conflict of interest.

Keywords

bilayer actuators, multicolor fluorescence, polymeric films, self-sustained oscillations

Received: January 11, 2021
Published online: February 1, 2021

---

[1] H. Wang, X. F. Ji, Z. T. Li, F. H. Huang, *Adv. Mater.* **2017**, *29*, 1606117.
[2] R. Gao, X. Y. Fang, D. P. Yan, *J. Mater. Chem. C* **2019**, *7*, 3399.
[3] S. X. Wei, W. Lu, H. Liu, J. Zhang, T. Chen, *Angew. Chem., Int. Ed.* **2020**, *59*, https://doi.org/10.1002/anie.202007506.
[4] T. Han, L. J. Liu, D. Wang, J. L. Yang, B. Z. Tang, *Macromol. Rapid Commun.* **2020**, *41*, 2000311.
[5] K. Meng, C. Yao, Q. M. Ma, Z. H. Xue, Y. P. Du, W. G. Liu, D. Y. Yang, *Adv. Sci.* **2019**, *6*, 1802112.
[6] Q. D. Zhu, K. V. Vliet, N. H. Andersen, A. Miserez, *Adv. Funct. Mater.* **2019**, *29*, 1808191.
[7] M. M. Li, Q. Q. Lyu, L. T. Sun, B. L. Peng, L. B. Zhang, J. T. Zhu, *ACS Appl. Mater. Interfaces* **2020**, *12*, 39665.
[8] X. Zhou, L. B. Wang, Z. C. Wei, G. S. Weng, J. He, *Adv. Funct. Mater.* **2019**, *29*, 1903543.
[9] W. Lu, C. X. Ma, D. Zhang, X. X. Le, J. W. Zhang, Y. J. Huang, C. F. Huang, T. Chen, *J. Phys. Chem.* **2018**, *122*, 9499.
[10] Q. Liu, T. H. Liu, Y. Fang, *Langmuir* **2020**, *36*, 2155.
[11] M. X. Xie, F. G. Xu, L. Z. Zhang, J. Yin, X. S. Jiang, *ACS Macro Lett.* **2018**, *7*, 540.
[12] Z. J. Wang, Z. Y. Ma, Y. Wang, Z. J. Xu, Y. Y. Luo, Y. Wei, X. R. Jia, *Adv. Mater.* **2015**, *27*, 6469.
[13] Y. Zhang, X. Le, Y. Jian, W. Lu, J. Zhang, T. Chen, *Adv. Funct. Mater.* **2019**, *29*, 1905514.
[14] W. Lu, J. T. Zhou, K. Y. Liu, D. Chen, L.i. M. Jiang, Z. Q. Shen, *J. Mater. Chem. B* **2013**, *1*, 5014.
[15] H. Y. Zheng, C. Y. Li, C. C. He, Y. Q. Dong, Q. S. Liu, P. F. Qin, C. Zeng, H. L. Wang, *J. Mater. Chem. C* **2014**, *2*, 5829.
[16] M. J. Feeney, S. W. Thomas, *Macromolecules* **2018**, *51*, 8027.
[17] H. Wang, X. F. Ji, Z. T. Li, C. N. Zhu, X. X. Yang, T. F. Li, Z. L. Wu, F. H. Huang, *Mater. Chem. Front.* **2017**, *1*, 167.
[18] J. K. Rad, A. R. Ghomi, K. Karimipour, A. R. Mahdavian, *Macromolecules* **2020**, *53*, 1613.
[19] A. Lavrenova, D. W. R. Balkenende, Y. Sagara, S. Schrettl, Y. C. Simon, C. Weder, *J. Am. Chem. Soc.* **2017**, *139*, 4302.
[20] C. X. Zhang, H. W. Li, Y. Q. Wu, *Macromol. Rapid Commun.* **2020**, *41*, 2000120.
[21] S. Tao, S. Zhu, T. Feng, C. Zheng, B. Yang, *Angew. Chem., Int. Ed.* **2020**, *59*, 9826.
[22] Y. H. Cheng, J. G. Wang, Z. J. Qiu, X. Y. Zheng, N. L. C. Leung, J. W. Y. Lam, B. Z. Tang, *Adv. Mater.* **2017**, *29*, 1703900.
[23] F. Li, X. D. Wang, Z. G. Xia, C. F. Pan, Q. L. Liu, *Adv. Funct. Mater.* **2017**, *27*, 1700051.

[24] R. N. Jia, W. G. Tian, H. T. Bai, J. M. Zhang, S. Wang, J. Zhang, *Nat. Commun.* **2019**, *10*, 795.

[25] L. D. Zhang, P. Naumov, *Angew. Chem., Int. Ed.* **2015**, *127*, 8766.

[26] L. Hu, Q. Zhang, X. Li, M. J. Serpe, *Mater. Horiz.* **2019**, *6*, 1774.

[27] C. Lv, H. Xia, Q. Shi, G. Wang, Y. S. Wang, Q. D. Chen, Y. L. Zhang, L. Q. Liu, H. B. Sun, *Adv. Mater. Interfaces* **2017**, *4*, 1601002.

[28] X. X. Le, W. Lu, J. W. Zhang, T. Chen, *Adv. Sci.* **2019**, *6*, 1801584.

[29] L. Liu, M. Wang, L. X. Guo, Y. Sun, X. Q. Zhang, B. P. Lin, H. Yang, *Macromolecules* **2018**, *51*, 4516.

[30] J. Q. Liao, M. Yang, Z. Liu, H. L. Zhang, *J. Mater. Chem. A* **2019**, *7*, 2002.

[31] S. X. Wei, W. Lu, X. X. Le, H. Lin, B. Y. Wu, J. W. Zhang, T. Chen, *Angew. Chem., Int. Ed.* **2019**, *58*, 16243.

[32] Z. Li, G. Wang, Y. Wang, H. Li, *Angew. Chem., Int. Ed.* **2018**, *57*, 2194;

[33] J. Wang, S. Sun, B. Wu, L. Hou, P. Ding, X. Guo, M. A. Cohen Stuart, J. Wang, *Macromolecules* **2019**, *52*, 8643.

[34] E. R. Trivedi, S. V. Eliseeva, J. Jankolovits, M. M. Olmstead, S. Petoud, V. L. Pecoraro, *J. Am. Chem. Soc.* **2014**, *136*, 1526.

[35] J. C. Lai, X. Y. Jia, D. P. Wang, Y. B. Deng, P. Zheng, C. H. Li, J. L. Zuo, Z. Bao, *Nat. Commun.* **2019**, *10*, 1164.

[36] K. Binnemans, *Chem. Rev.* **2009**, *109*, 4283.

[37] W. Lu, P. Xiao, Z. Liu, J. Gu, J. Zhang, Y. Huang, Q. Huang, T. Chen, *ACS Appl. Mater. Interfaces* **2016**, *8*, 20100.

[38] Q. Yin, S. Tu, M. Chen, L. Wu, *Macromol. Mater. Eng.* **2020**, *305*, 2000013.